Biosensors and Bioelectronics 32 (2012) 163–168

Contents lists available at SciVerse ScienceDirect

Biosensors and Bioelectronics

journal homepage: www.elsevier.com/locate/bios

Label-free and reagentless electrochemical detection of PCR fragments using self-assembled quinone derivative monolayer: Application to *Mycobacterium tuberculosis*

Q.D. Zhang [a], G. March [a], V. Noel [a], B. Piro [a], S. Reisberg [a], L.D. Tran [a,b], L.V. Hai [a], E. Abadia [d], P.E. Nielsen [c], C. Sola [d,e], M.C. Pham [a,*]

[a] *Interfaces, Traitement, Organisation et Dynamiques des Systèmes (ITODYS), UMR CNRS 7086, Université Paris Diderot, Sorbonne Paris Cité 15 rue Jean Antoine de Baïf, 75205 Paris Cedex 13, France*
[b] *Institute of Material Sciences (IMS), Vientamese Academy of Science and Technology, 18 Hoang Quoc Viet, Hanoi, Viet Nam*
[c] *Department of Cellular and Molecular Medicine, The Panum Institute, Blegdansvej 3 C, DK-2200 Copenhagen, Denmark*
[d] *Infection, Génétique, Evolution des Pathogènes Emergents, Institut de Génétique et Microbiologie, IGM UMR CNRS 8621, Bât. 400, 91405 ORSAY Cedex, France*
[e] *Unité de Génétique Mycobactérienne, Institut Pasteur, France*

ARTICLE INFO

Article history:
Received 9 March 2011
Received in revised form
29 September 2011
Accepted 30 November 2011
Available online 7 December 2011

Keywords:
Self-assembled monolayers
DNA biosensor
Label-free
Reagentless
Signal-on
PCR product
Mycobacterium tuberculosis

ABSTRACT

We report a signal-on, label-free and reagentless electrochemical DNA biosensor, based on a mixed self-assembled monolayer of thiolated hydroxynaphthoquinone and thiolated oligonucleotide. Electrochemical changes resulting from hybridization were evidenced with oligonucleotide targets (as models), as well as with polymerase chain reaction (PCR) products related to different lineages of *Mycobacterium tuberculosis* strains. With pure oligonucleotides, this system achieves high sensitivity (~300 pM of DNA target, i.e. 30 fmol in a 100 μL sample) and excellent selectivity, allowing to detect a single mismatch on a sequence of 20 bases. With PCR products, current changes are specific to the bacterial strain from which the PCR fragment is produced. In addition, the sensor response is of the signal-on type, giving a positive signal change upon hybridization, and therefore does not suffer from false positive responses due to non-specific adsorption of DNA.

Electrochemical transduction offers great advantages over optical transduction systems which require fluorescent or chemiluminescent labels (Xu and Bard, 1995; Epstein et al., 2002; Calvo-Munoz et al., 2005) as it allows miniaturization and low-cost detection. This is why direct electrochemical DNA biosensors, which require neither modification of the target nor addition of a reagent to detect hybridization, are of great interest. The main aim is to find sensitive interfaces with charge transfer properties that change when hybridization occurs. This is based on difference between the physical properties of single-stranded DNA (ssDNA) and double-stranded DNA (dsDNA) (Piro et al., 2007; Thompson et al., 2003). Following this approach, a new direction is to fabricate biosensitive interfaces using self-assembled monolayers (SAM) (Gooding and Garry, 2005) which allows the physicochemical properties of the interfaces to be fine-tuned. Different research groups have used a similar approach in grafting a thiolated ssDNA (that can adopt a stem-loop structure in some formats) modified by an electroactive ferrocene tag (Anne et al., 2003; Fan et al., 2003). Before target addition, the ferrocene tag, close to the electrode surface generates an amperometric current. After target addition, the rigid duplex moves the ferrocene tag away from the electrode surface, so no current is observed. The detection limit reached by the hairpin system is good (10 pM) (Fan et al., 2003). Nevertheless, the transduction results in an "off" signal with the current decreasing upon hybridization. In the field of label-free sensors, signal-on (current increase) devices are preferable to signal-off ones, in that false positives are less likely. Signal-on architectures using this approach have been developed (Ricci and Plaxco, 2008; Lubin and Plaxco, 2010) notably a system based on a DNA-poly(ethylene glycol)-DNA triblock probe which can operate with target concentrations up to 200 pM (Immoos et al., 2004). Another example is the use of an immobilized double (pseudoknot) or triple stem-loop DNA probe modified at its 3′-terminus with methylene blue,

* Corresponding author. Tel.: +33 1 57277223; fax: +33 1 44276814.
E-mail addresses: mcpham@univ-paris-diderot.fr, mcpham@paris7.jussieu.fr (M.C. Pham).

0956-5663/$ – see front matter © 2011 Elsevier B.V. All rights reserved.
doi:10.1016/j.bios.2011.11.048

where detection limits of 2 nM and 5 nM respectively have been reported (Xiao et al., 2007, 2009). Finally, another "signal-on" architecture is based on a target-induced strand displacement, where target binding generates a short, flexible ssDNA modified with methylene blue. Sub-picomolar detection has been reported (Xiao et al., 2006). All these systems use the same transduction principle based on the variation of the distance between a redox tag attached to the probe strand and the electrode surface.

We have adopted a different approach, which requires no redox tag, where electroactive layers based on quinone derivatives are used. It was demonstrated that hydroxy-naphthoquinones, in the Electronic Conducting Polymer configuration, present significant potential for DNA sensors (Reisberg et al., 2005, 2006; Pham et al., 2003). More recently, we have investigated the electroactivity of a 5-hydroxy-3-hexanedithiol-1,4-naphthoquinone monolayer (JUG_{SH}) self-assembled on gold (March et al., 2008a). These results show that JUG_{SH} electroactivity is very sensitive to the presence of DNA in its vicinity and that JUG_{SH} is therefore able to act as a sensitive monolayer for label-free and reagentless electrochemical biosensing of DNA hybridization. The transduction principle was not clearly defined and we previously assumed that physicochemical interactions (hydrogen bond interactions, weak interactions or electrostatic ones) between DNA strands and the immobilized naphthoquinone are central to the detection scheme.

In this paper, we pursue the description of this new class of label-free DNA sensors by identifying factors controlling the direct transduction efficiency and by assessing its ability to detect short oligonucleotides in a complex real sample consisting of PCR-amplified fragments. We used first peptide nucleic acids (PNAs) as probes because these DNA homologues have the same steric hindrance and the same hybridization capabilities but, since they are neutral, do not exert electrostatic charge effects on their environment. It is therefore possible to conclude whether charges carried by nucleotide strands (DNA) are implied in the electrochemical transduction process. Secondly, we report results obtained not only with oligonucleotide targets (as models), but with *real-world* PCR products (Bettazzi et al., 2008; Farabullini et al., 2007; Del Giallo et al., 2005). For this, we use PCR products related to different lineages (of different geographical origin) and strains (quoted as a number in brackets for each lineage) of *Mycobacterium tuberculosis*. Strains of three different lineages were investigated: M. africanum (51), Beijing (23), Latino-America and Mediterranean LAM (1). It is shown that current changes are specific to the target sequence, that is, of the lineage and strain from which the PCR residue is produced. The identification of *M. tuberculosis* at the lineage level could be considered as a surrogate marker for tuberculosis drug resistance and is important for patient treatment choice

1. Experimental

1.1. Materials

5-Hydroxy-1,4-naphthoquinone (JUG) and phosphate buffer solution (PBS) were purchased from Aldrich and Sigma, respectively. Aqueous solutions were made with Milli-Q water. Ethyl acetate was purchased from VWR. 5-Hydroxy-3-hexanedithiol-1,4-naphthoquinone (JUG_{SH}) was synthesized in the laboratory according to a published procedure (March et al., 2008a). Oligonucleotides were synthesized by Eurogentec (Belgium). Peptide nucleic acids (PNA) were synthesized in the Department of Cellular and Molecular Medicine, Panum Institute, Denmark. Three formats of hybridization were envisaged on the JUG_{SH} system: DNA probe-DNA target, PNA probe-DNA target and DNA probe-DNA (from PCR) target. Sequences are given with the bases really used in bold; others are spacers to avoid edge effects, and mismatches are underlined: DNA probe (DNA-SH): SH-C_6H_{12}-3′ TCC GA**T CTT CCT CTC TCT ACC CAC G** CT 5′; PNA probe (PNA-SH) SH-C_6H_{12}-Gly-3′ **T CTT CCT CTC TCT ACC CAC G** –$(eg_2)_3$-Cys-Ac 5′; complementary DNA target (HIV) 5′ **A GAA GGA GAG AGA TGG GTG C** 3′; single mismatch target (M-HIV) 5′ **A GAA GGA GAG AAA TGG GTG C** 3′; random target (RAND) 5′ **A TCA ACT TCC TAG TAA ATG C** 3′. For hybridization with PCR fragments, the probe sequence is Sp32-SH, SH C_6H_{12} 3′ ACT TGT GCG GCT ATG GAT AAA CCA G 5′; complementary to the so-called Spacer 32 sequence (5′-TGA ACA CGC CGA TAC CTA TTT GGT C-3′) present in the CRISPR[1] spacer sequence from M. africanum and the Latino American-Mediterranean (LAM) clinical isolates, whereas the PCR product from the Beijing strain does not present any complementarity with this probe sequence (Sebban et al., 2002).

1.2. Electrochemical materials and methods

Electrodes were ultrasonicated for several minutes in acetone and ethanol and finally put inside an UV-Ozone cleaner (5 min) before SAM assembling. A conventional one-compartment, three-electrode cell was used with an Autolab PGSTAT 100. The SAM-modified electrodes were tested using 1 cm^2 platinum flag auxiliary electrode and a SCE reference electrode. Hybridization was detected by following the modification of the quinone electroactivity using Square Wave Voltammetry (SWV), in order to minimize the capacitive component of the current. The following parameters were used: pulse height 50 mV, pulse width 50 ms, scan increment 2 mV, frequency 12.5 Hz, potential range (−0.65 V; −0.2 V vs. SCE). The SWV scans were recorded in PBS medium, bubbled with argon for 20 min before the first measurement, to remove oxygen, which is known to interact with quinone. Up to five CVs or square wave voltammograms were performed for each measurement until complete stabilization of the signal. This procedure is necessary to ensure a good reproducibility in different experiments.

Polycrystalline gold electrodes (supplied by BASi, area: 0.03 cm^2) were used as working electrodes.

See Supplementary Information file for PCR details.

1.3. Monolayer formation

Polycrystalline gold electrodes (radius 1 mm) were sequentially polished on polishing clothes (Struers, Denmark) with diamond pastes of decreasing particle size, followed by ultrasonication for several minutes in acetone and ethanol. They are then potential scanned from −0.3 to 1.5 V at 50 mV s^{-1} in 0.5 M aqueous H_2SO_4. The electroactive self-assembled monolayers were obtained by immersing the freshly cleaned Au electrode in 1 mg mL^{-1} JUG_{SH} in ethyl acetate solution overnight with stirring in an argon atmosphere.

1.4. DNA or PNA grafting and hybridization procedures

50 μL of 4 μM probes in PBS having the 3′-alkylthiol functionality (DNA-SH, PNA-SH or Sp32-SH) were placed on a JUG_{SH}-modified gold electrode overnight for self-assembly. The electrodes obtained in this way (modified with a mixed monolayer of JUG_{SH}/probe) were then rinsed with PBS (pH 7.4) before use.

In the case of the single mismatched sequence (M-HIV), hybridization was performed at 50 °C and the mixture was slowly cooled to 37 °C. For PCR fragments, 15 μL of the PCR products diluted in 225 μL of PBS was first denatured at 95 °C for 60 min, then slowly cooled to 55 °C and left for 2 h at 55 °C to hybridize. Finally,

[1] Clustured Regularly Interspersed Palindromic Repeats.

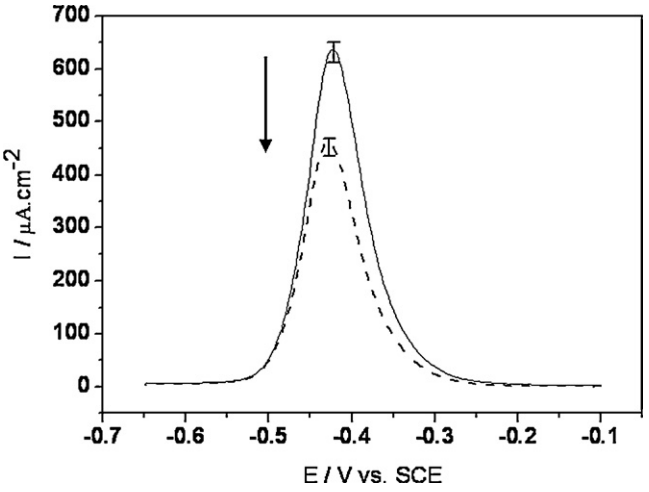

Fig. 1. SWV of JUG_{SH} before (solid line) and after (dashed line) DNA probe grafting.

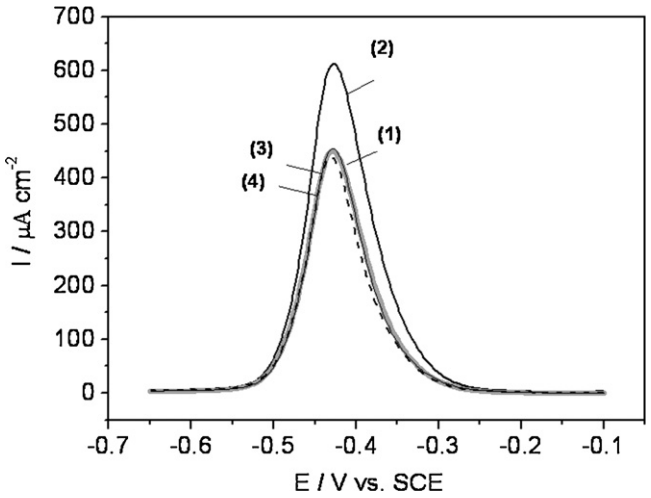

Fig. 2. SWV peaks obtained for electrode before hybridization (curve 1, dashed line) then after hybridization with the full-complementary sequence (HIV, curve 2); after addition of a single-mismatch (M-HIV, curve 3, gray) or a random sequence (RAND, curve 4, black).

the electrode was immersed in PBS for 1 h at room temperature in order to remove non-hybridized targets.

2. Results and discussion

2.1. Experiments with synthetic DNA

The pure JUG_{SH} monolayer was analyzed by square-wave voltammetry (SWV) in PBS between −0.2 V and −0.65 V vs. SCE (Fig. 1, continuous line). One oxidation peak, corresponding to the quinone redox process, appears at ca. −0.45 V. In the following, the change in intensity of this peak current will be considered as the significant parameter for probe grafting and hybridization experiments. As the hybridization procedure involves heating at 50 °C, the stability of JUG_{SH} was studied at this temperature. After 2 h in PBS, the SWV peak current shows a 10% decrease (see SI 1) which we assume to be due to the low thermal stability of the JUG_{SH} monolayer.

The mixed DNA/JUG_{SH} monolayer was obtained by immersing a pure JUG_{SH} monolayer in a 1 μM DNA-SH solution for 18 h at room temperature. We assume that the mixed monolayer is obtained by partial replacement of JUG_{SH} by the thiolated DNA-SH probes. The total charge of the monolayer, measured by cyclic voltammetry experiments, is not significantly changed by probe grafting; this indicates that very few JUG_{SH} molecules are removed from the surface (see SI 2). Previous fluorescence experiments indicated that this self-assembling set-up gives a surface probe density of 10 pM cm^{-2} (Xiao et al., 2006). However, although the amount of probe immobilized on the SAM is not sufficient to noticeably alter the total juglone surface concentration, SWV experiments show that probes grafting reduce the current density (Fig. 1, dashed line). The decrease in SWV peak currents will be expressed as the relative current variation upon grafting ($\Delta R_g = 100 \times (I_a - I_b)/I_a$ where I_a and I_b are the current densities after and before probe grafting respectively). This value is $-30 \pm 5\%$.

For hybridization experiments, solutions containing 0.1 μM targets were used. Note that the mismatch sequence M-HIV was hybridized at 50 °C instead of room temperature to improve selectivity. More than 100 samples were used for this study. SWV results are presented in Fig. 2; curve 1 is that for an electrode before hybridization (dashed line). Addition of the complementary target (HIV) leads to a clear current increase (curve 2) with $\Delta R_h = +35 \pm 5\%$ where $\Delta R_h = 100 \times (I_c - I_a)/I_a$, I_c being the current density after target addition. On the contrary, addition of the random target (RAND, curve 3) or M-HIV (curve 4) does not lead to a significant current change. At first sight, the similar behavior for hybridization with random and mismatch seems to be abnormal, but it should be recalled that the hybridization conditions are not the same with these two targets. In order to minimize non-specific hybridization, the mismatch sequence was hybridized at 50 °C. These hybridization conditions were previously determined using fluorescein-modified DNA sequences (Reisberg et al., 2010).

This sensor exhibits signal-on detection, as the current increases upon hybridization with the complementary target. Moreover, its selectivity is excellent, allowing discrimination of a single-base mismatch.

To investigate the detection limit of the system, the SWV current response was measured as a function of the complementary target (HIV) concentration. Results are shown in Fig. 3 for six different concentrations between 30 pM and 100 nM (see SI 3 for the log. display). We recorded the relative current variation ($\Delta I/I$) obtained when a non-complementary strand is added at 100 nM, this concentration is also used in the case of the perfect match. In such condition, we obtained $\Delta I/I = 0 \pm 3\%$. We assume that all current variation exceeding +3% are significant. Hence, the detection threshold estimated is ca. 300 pM ($5\% < \Delta I/I < 7\%$); that is better than most literature values for direct electrochemical DNA biosensors (10^{-9} and 10^{-10} M) (Sassolas et al., 2008). Compared with the detection threshold reported for signal-on systems using also

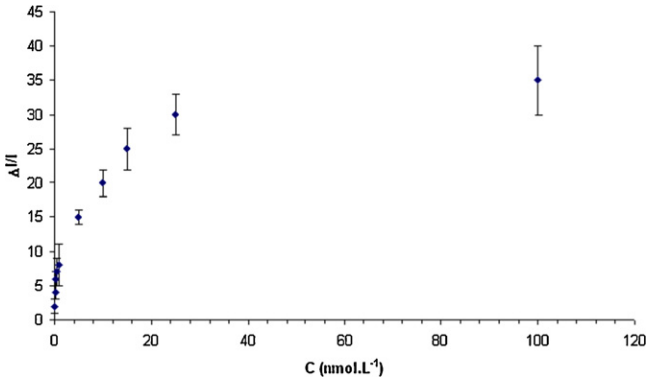

Fig. 3. Relative current density difference ΔR_h (expressed as the difference between the current after and before hybridization normalized to the current before hybridization), measured for different HIV concentrations.

transduction based on conformational change of DNA probe upon hybridization, our system is in the same range: 200 pM for the DNA-polyethylene glycol-DNA triblock probe-based system (Immoos et al., 2004) and a few nM for the double or triple stem-loop DNA probe-based architecture (Xiao et al., 2007, 2009). Only that based on target-induced strand displacement is better, at 400 fM (Xiao et al., 2006).

Concerning the reproducibility of the results, the standard deviations here could appear high according to well-known analytical standards. However, it falls in a common range when compared to other reagentless DNA biosensors. Moreover, the system is "signal-on" so less sensitive to false positives.

2.2. Transduction mechanism

The ability to modulate the electroactivity of the JUG_{SH} layer by hydrogen bonding (March et al., 2008b) and the specific capacity of the grafted DNA probe to interact with the monolayer surface suggest an interpretation of the signal-on behavior upon hybridization. Before hybridization, the single strand behaves as a random coil (Ortiz et al., 1998; Armitage et al., 1998), which has a high degree of freedom and can interact with JUG_{SH} through hydrogen bonds. This increases the activation energy of the redox reaction, so that it slows down the reaction rate and lowers the related current (March et al., 2008b). This explains the decrease in the observed SWV peak current when the probe strand is grafted. The absence of peak shift, usually encountered in the case of strong hydrogen bonding, indicates that the formal potential is constant. Hence, this means that interactions with DNA are equally shared on the oxidized and reduced forms. This characteristic behavior of the JUG_{SH} monolayer has been discussed in a previous paper (March et al., 2008b). Only the electron transfer rate depends on the JUG_{SH}/DNA probe interactions. When the complementary target is added, a double helix is formed, which weakens the single strand/JUG_{SH} interactions and leads to an increase in the JUG_{SH} redox rate. However, the above discussion does not take into account the negative charge on the phosphodiester DNA backbone. Experiments with peptide nucleic acids could give information about the relative importance of hydrogen bonding and electrostatic effects in the transduction mechanism. The juglone monolayer carries a negative surface charge due to the deprotonation of the hydroxyl function for pHs above 7 (March et al., 2008b). Hence, most of the hydroxyl groups are deprotonated at pH 7.4. In order to investigate the contribution of electrostatic interactions in the transduction process, experiments where carried out with PNA homologues which have the same steric hindrance and the same hybridization capabilities as DNA but, since they are neutral, exert much less electrostatic effects (Uhlmann et al., 1998; Nielsen et al., 1991).

2.3. Experiments with peptide nucleic acids (PNAs)

After insertion of the PNA-SH probe into the pure JUG_{SH} monolayer, the quinone surface content is not significantly altered, as shown by cyclic voltammetric control experiments. We assume that the mechanism of mixed monolayer formation occurs is the same for DNA-SH, leading to almost the same surface density. Indeed, this is mainly controlled by the length of the alkylthiol (Ulman, 1998), which is the same for PNA-SH and DNA-SH (see Section 1).

The typical SWV of JUG_{SH} after PNA-SH probe immobilization is similar to that for DNA-SH (Fig. 4): the peak current decreases, $\Delta R_g = 65 \pm 5\%$, higher than with DNA, and the peak goes to slightly higher potential. Therefore, it seems that the interaction between juglone and the PNA probe is stronger than with DNA.

Besides the fact that PNA grafting leads to a much more severe current density drop than DNA (see Figs. 1 and 4), the increase upon hybridization is also significantly higher in the PNA/DNA configuration than in the DNA/DNA one. Fig. 5 presents SWV responses of a PNA/JUG_{SH}-modified electrode after incubation with the complementary DNA sequence. A large current increase is detected, $\Delta R_h = +55 \pm 15\%$. Incubation with the non-complementary and the mismatch sequences does not lead to any significant current increase (see SI 4).

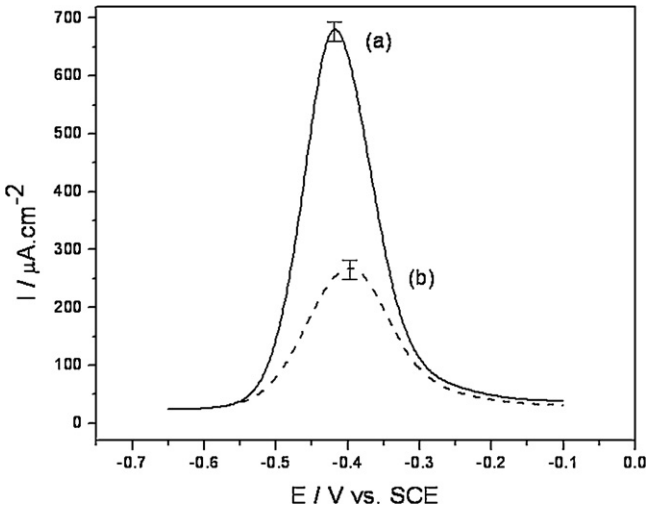

Fig. 4. SWV current density response of a JUG_{SH} Au electrode without PNA probe (a) and after PNA probe grafting (b).

In the mixed monolayer (DNA—JUG_{SH} or PNA—JUG_{SH}), JUG_{SH} could form hydrogen bonds with DNA probes as well as with PNA. Since it is neutral, PNA is more likely to interact with JUG_{SH}, which is negatively charged at pH 7.4 (March et al., 2008b), than the polyanionic DNA.

Single-stranded PNA and DNA are sterically similar both being random coils of short polymer chains (Ortiz et al., 1998; Armitage et al., 1998; Juhn et al., 2001). Hence, single stranded DNA or PNA has a high degree of freedom (in our case, increased by the length and the flexibility of the alkylthiol linker) and is able to interact with molecules on the surface. Conversely, as the double strand (DNA/DNA or PNA/DNA) is rigid and straight, hydrogen-bonding interactions with JUG_{SH} are disrupted. The fact that the JUG_{SH} electroactivity is modulated by hydrogen bonding and that the grafted

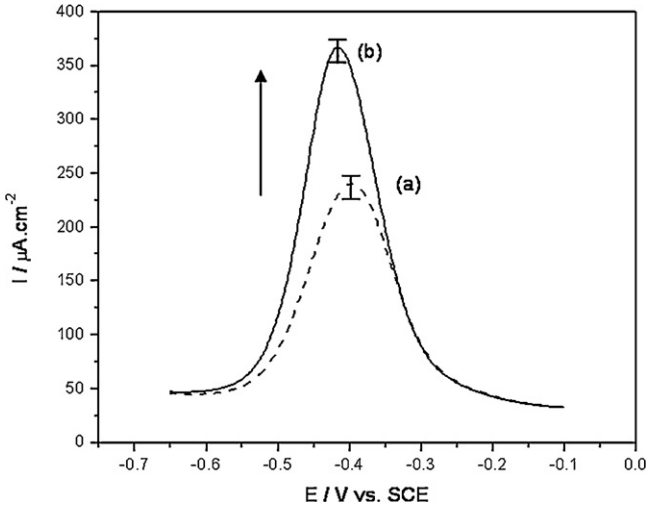

Fig. 5. SWV current density response of PNA/JUG_{thio}-modified electrode (a); after hybridization with the HIV target (b).

DNA or PNA probes can interact with the monolayer suggests an interpretation of the signal-on behavior following hybridization. Before hybridization, the single-stranded DNA or PNA probe can interact with JUG_{SH} and slows down the redox reaction, explaining the decrease in SWV current density upon probe grafting. After complementary target addition, the double helix disrupts the single-stranded DNA or PNA/JUG_{SH} interactions so the JUG_{SH} redox rate increases. Indeed, our previous work has shown that the rupture of hydrogen bonds increases the apparent rate constant of the JUG_{SH} redox reaction at biological pH.

To get deeper insight into the transduction mechanism, a crucial parameter, the distribution of DNA probes inside the juglone monolayer, has to be controlled. That is why we are currently working with nanostructured substrates allowing the construction of well defined mixed monolayers. We plan to study several parameters such as the ratio of juglone to DNA probes, and to develop a theoretical approach in order to correlate the strength of the hydrogen-bonding interaction and the juglone electron transfer rate. All these points are currently under investigation.

This study already shows that our system is able to detect, with excellent sensitivity, short synthetic DNA targets. In the following, it will be evaluated for its capability to detect longer sequences in PCR products.

2.4. Hybridization with PCR products

Experiments were extended to assays on PCR products related to *M. tuberculosis*. These products have 200 bases in average, with a sequence of 25 bases, specific for the targeted bacteria strain. This experimental section details these lineages and strains, and shows whether or not they contain the target sequence (Spacer32). One of the main difficulties lies in the use of a complex sample containing very long DNA sequences for which non-specific hybridization may occur.

To probe the specificity of our sensor, we used salmon genomic DNA that contains a large variety of strand lengths (between 200 and 800 bp) along with other targets in a mixture for which the exact ODN concentration is known. Hybridization solutions were first heated at 95 °C for 1 h, to allow denaturation, then cooled to 55 °C for 2 h. A current increase was observed when the complementary target (25 bp at 0.1 μM) is present in the mixture; there is no significant variation without it (see SI 5). The non-specific hybridization content can be estimated from the known exact target concentration in the mixture. We obtained a 18% current increase, vs. 22% for DNA target alone in PBS solution. We, therefore, estimate the contribution of non-specific hybridization to the signal increase to be below 4% at 55 °C.

The electrodes were modified as already explained above with JUG_{SH} and the Sp32-SH probe sequence. Fig. 6 shows SWV current densities obtained with an electrode before hybridization, then after incubation with PCR products from M. africanum (51) and LAM (1). A positive current response is observed for M. africanum (51) ($\Delta R_h = 23 \pm 5\%$) and LAM (1) ($\Delta R_h = 25 \pm 6\%$), but no significant increase is observed for Beijing (23) ($\Delta R_h = 5 \pm 2\%$) or for pure PBS, as expected (see SI 6). These responses fit very well with the presence or not of the Sp-32 target.

Current changes are lower than those obtained for synthetic DNA. This can be due both to the uncertain concentration of the PCR product and the greater steric hindrance of these PCR sequences compared to the shorter oligonucleotides. Beside these two factors, the weaker electrochemical signal for PCR amplicons could be ascribed to their reannealing, a process competing with hybridization with the specific DNA on the surface. Hybridization in solution is easier than on a solid support, although the sequences are longer (200 bp vs. 25 bp).

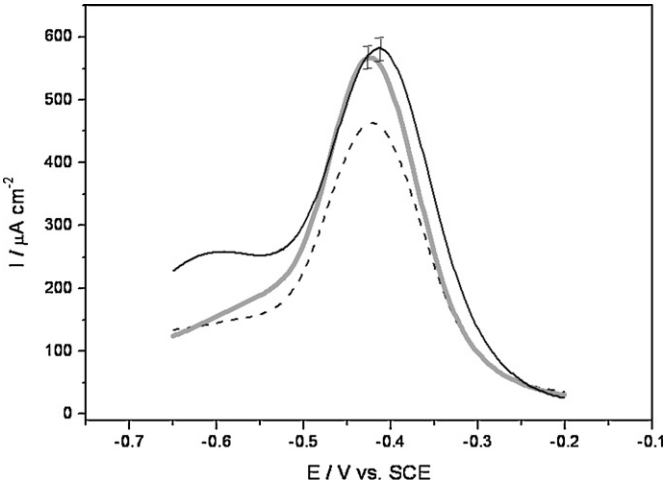

Fig. 6. SWV peaks obtained for electrode before hybridization (dashed line), then after hybridization with PCR products from africanum (51) (gray) or with PCR products from LAM (1) (black).

3. Conclusions

We have demonstrated that JUG_{SH} is an interesting system for making a label-free electrochemical sensor allowing signal-on detection. It leads to very good sensitivity and selectivity, as reported in previous work, when short synthetic oligonucleotides are used. In order to investigate the transduction mechanism, in this work, neutral PNAs were compared with the charged DNAs. Our results indicate that the hydrogen-bonding between the probe and the electroactive JUG_{SH} monolayer are the key parameter that controls the signal variation upon hybridization. They are weaker with DNA than PNA, due to the repulsive electrostatic interaction between the anionic JUG_{SH} and the polyanionic DNA. This is evidenced by the difference in sensor response when DNA probes are replaced by PNA.

A good detection threshold 300 pM target was obtained for synthetic DNA. The system was then extended to analyze real-world PCR products. In this case, our study offers valuable results concerning the hybridization of longer DNA fragments with short DNA probes. PCR products related to different lineages and strains of *M. tuberculosis* were used. Current changes are specific to the bacterial strain from which the PCR fragment is produced. This label-free electrochemical system can therefore be extended to numerous other applications where the CRISPR strategy is used.

Acknowledgements

Q.D. Zhang and G. March thank the French Ministry of Research for a Ph.D. grant. L.V. Hai thanks the Vietnamese Ministry of Education and Training for a Ph.D. grant. The University of Paris-Sud 11 is also warmly thanked for the post-doctoral grant to E. Abadia. ITODYS and IGEPE thank the French General Delegation for Armaments (DGA) for financial support.

Appendix A. Supplementary data

Supplementary data associated with this article can be found, in the online version, at doi:10.1016/j.bios.2011.11.048.

References

Anne, A., Bonnaudat, C., Demaille, C., Wang, K., 2003. J. Am. Chem. Soc. 125, 1112–1113.
Armitage, B., Ly, D., Koch, T., Frydenlung, H., Orum, H., Schuster, G.B., 1998. Biochemistry 37, 9417–9425.

Bettazzi, F., Lucarelli, F., Palchetti, I., Berti, F., Marrazza, G., Mascini, M., 2008. Anal. Chim. Acta 614, 93–102.
Calvo-Munoz, M.L., Dupont-Filliard, A., Billon, M., Guillerez, S., Bidan, G., Marquerette, C., Blum, L., 2005. Bioelectrochemistry 66, 139–143.
Del Giallo, M.L., Lucarelli, F., Cosulich, E., Pistarino, E., Santamaria, B., Marrazza, G., Mascini, M., 2005. Anal. Chem. 77, 6324–6330.
Epstein, J.R., Biran, I., Walt, D.R., 2002. Anal. Chim. Acta 469, 3–36.
Fan, C., Plaxco, K.W., Heeger, A., 2003. Proc. Natl. Acad. Sci. U.S.A. 100, 9134–9137.
Farabullini, F., Lucarelli, F., Palchetti, I., Marrazza, G., Mascini, M., 2007. Biosens. Bioelectron. 22, 1544–1549.
Gooding, J.J., Garry, C.K., 2005. J. Mater. Chem. 15, 4876–4880.
Immoos, C.E., Lee, S.J., Grinstaff, M.W., 2004. J. Am. Chem. Soc. 126, 10814–10815.
Juhn, H., Demidov, V.V., Coull, J.M., Fiandaca, M.J., Gildea, B.D., Frank-Kamenetskii, M.D., 2001. Antisense Nucleic Acid Drug Dev. 11, 265–270.
Lubin, A.A., Plaxco, K.W., 2010. Acc. Chem. Res. 43, 496–505.
March, G., Noel, V., Piro, B., Reisberg, S., Pham, M.C., 2008a. J. Am. Chem. Soc. 130, 15752–15753.
March, G., Reisberg, S., Piro, B., Pham, M.-C., Delamar, M., Noel, V., Odenthal, K., Hibbert, D., Gooding, J.J., 2008b. J. Electroanal. Chem. 622, 37–43.
Nielsen, P.E., Egholm, M., Berg, R.H., Buchardt, O., 1991. Science 254, 1497–1500.
Ortiz, E., Estrada, G., Lizardi, P.M., 1998. Mol. Cell. Probes 12, 219–226.
Pham, M.C., Piro, B., Tran, L.D., 2003. Anal. Chem. 75, 6748–6752.
Piro, B., Reisberg, S., Noel, V., Pham, M.C., 2007. Biosens. Bioelectron. 22, 3126–3631.
Reisberg, S., Piro, B., Noel, V., Pham, M.C., 2005. Anal. Chem. 77, 3351–3356.
Reisberg, S., Piro, B., Noel, V., Pham, M.C., 2006. Bioelectrochemistry 69, 172–179.
Reisberg, S., Acevedo, D.F., Korovitch, A., Piro, B., Noel, V., Buchet, I.##l., Tran, L.D., Barbero, C.A., Pham, M.C., 2010. Talanta 80, 1318–1325.
Ricci, F., Plaxco, K.W., 2008. Microchim. Acta 163, 149–155.
Sassolas, A., Leca-Bouvier, B.D., Blum, L., 2008. Chem. Rev. 108, 109–139.
Sebban, M., Mokrousov, I., Rastogi, N., Sola, C., 2002. Bioinformatics 18, 235–243.
Thompson, L.A., Kowalik, J., Josowicz, M., Janata, J., 2003. J. Am. Chem. Soc. 125, 324–325.
Uhlmann, E., Peyman, A., Breipohl, G., Will, D.W., 1998. Angew. Chem. Int. Ed. 37, 2796–2823.
Ulman, A., 1998. Self-Assembled Monolayers of Thiols (Thin Films). Academic Press.
Xiao, Y., Lubin, A.A., Baker, B.R., Plaxco, K.W., Heeger, A.J., 2006. Proc. Natl. Acad. Sci. 103, 16677–16680.
Xiao, Y., Qu, X., Plaxco, K.W., Heeger, A.J., 2007. J. Am. Chem. Soc. 129, 11896–11897.
Xiao, Y., Lou, X., Uzawa, T., Plakos, K.J.I, Plaxco, K.W., Soh, H.T., 2009. J. Am. Chem. Soc. 131, 15311–15316.
Xu, X.-H., Bard, A.J., 1995. J. Am. Chem. Soc. 117, 2625–2631.